Article ID: 1007-4627(2015) 04-0421-07

Study on the Capture and Acceleration Efficiency in HIAF-CRing

SHANG Peng[1,2], YIN Dayu[1], XIA Jiawen[1], YANG Jiancheng, QU Guofeng[1,2], ZHENG Wenheng[1,2], LI Zhongshan[1,2], RUAN Shuang[1,2]

(*1. Institute of Modern Physics, Chinese Academy of Sciences, Lanzhou 730000, China;*
2. University of Chinese Academy of Sciences, Beijing 100049, China)

Abstract: To reduce the beam loss during the capture and acceleration processes of CRing in HIAF project, the longitudinal beam motion is investigated using the typical ion of $^{238}U^{34+}$during the two processes mentioned above. The ions will be captured adiabatically firstly and then will be accelerated from 800 to 1130 MeV/u with a high efficiency using optimized RF voltage and RF phase program. After that the bunched beam will be debunched for the later beam compression. Simulation of these processes by tracking appropriate distributions with the longitudinal beam dynamics code ESME has been used to find optimum parameters such as RF phase, RF voltage. The variation of the parameter during the RF cycle and the character parameters of the RF cavity are presented.

Key words: simulation; HIAF; compression; adiabatic capture; acceleration

CLC number: TL5 **Document code:** A **DOI:** 10.11804/NuclPhysRev.32.04.421

1 Introduction

The HIAF (**H**igh **I**ntensity heavy ion **A**ccelerator **F**acility) project, which consists of a high intensity ion source SECR (Superconducting Electron Cyclotron Resonance), a high intensity Heavy Ion Linac (iLinac), a Booster Ring (BRing), a high precision Spectrometry Ring (SRing), a Compression Ring (CRing), an Energy Recovery Linac (ERL) and a multifunction storage ring system for heavy ion related researches, has been proposed by IMP (Institute of Modern Physics, Chinese Academy of Sciences) from the year 2009[1]. It's primary structure is shown in Fig. 1 .

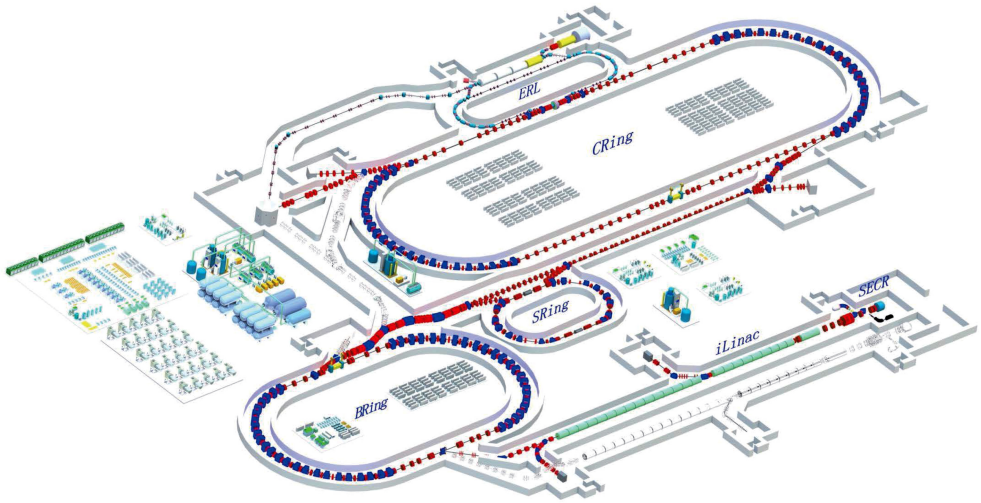

Fig. 1 (color online) The layout of HIAF project.

Received date: 14 Nov. 2014; **Revised date:** 8 Jan. 2015

Biography: SHANG Peng(1989–), male, Lanzhou, postgraduate, studying in the field of accelerator physcs: longitudinal dynamics; E-mail: shangpeng@impcas.ac.cn

Corresponding author: YIN Dayu, E-mail: yindy@impcas.ac.cn.

As an important component of the HIAF complex, the synchrotron CRing, see in Fig. 1, has been designed to be a multi-function accelerator with a maximum magnetic rigidity of 43 Tm. The basic parameters are listed in Table 1.

Table 1 Machine parameters for CRing.

Parameter	Sign/unit	Value
Circumference	C_0/m	804
Average Radius	R/m	127.96
Bending Radius	ρ/m	19.11
Max. Magnetic Induction	$B_{\max}$/T	2.25
Max. Magnetic Rigidity	$B\rho$/Tm	43
Max. Ramping Rate	$\dot{B}_{\max}$/(T/s)	1.125
Initial Momentum Spread	$\Delta P/P$	$\pm 5\times 10^{-4}$
Gamma Transition	$\gamma_{\rm t}$	11.14

The injected beam which comes from BRing will firstly be accumulated into high intensity by an individual barrier bucket accumulation system. Then, the accumulated beam will be changed into a coasting beam and be captured into a stationary bucket adiabatically afterwards. The captured beam will be accelerated to a designed energy and then be compressed into a higher intensity. The high intensity beam will be extracted to internal and external target for the experiments eventually.

The capture efficiency and acceleration efficiency on CRing are studied in detail here with the code ESME. We only consider a typical ion of $^{238}U^{34+}$ in our simulations. The initial energy for the $^{238}U^{34+}$ beam is 800 MeV/u and it can be accelerated to the top energy of 1 130 MeV/u. The longitudinal beam dynamics code ESME has been developed to model those aspects of beam behavior in a synchrotron that are governed by the radio frequency systems. It follows the evolution of a macro-particle distribution in longitudinal phase space by iterating a map corresponding to the single-particle equations of motion[2].

The single particle equations for longitudinal motion in a synchrotron are naturally formulated as a pair of first order differential equations[3]:

$$\begin{cases} \dfrac{\mathrm{d}}{\mathrm{d}t}\left(\dfrac{\Delta E}{\omega_{\rm s}}\right)=\dfrac{q}{2\pi}\left[V(\theta)-V(\theta_{\rm s})\right] \\ \dfrac{\mathrm{d}}{\mathrm{d}t}\Delta\theta=-\dfrac{h\omega_{\rm s}\eta}{\beta^2 E}\Delta E \end{cases} . \tag{1}$$

Eqs. (1) are used as a basic theory in computation. Here, $\Delta E=E-E_{\rm s}$, $\Delta\theta=\theta-\theta_{\rm s}$, $\eta=1/\gamma^2-1/\gamma_{\rm t}^2$ with $\gamma_{\rm t}$ the Lorentz factor at transition energy. E and θ refer the total energy and the phase of the particle. $V(\theta)=V\cdot\sin(\theta)$, where V is the instantaneous RF voltage, it is equivalent to $V(t)$. ω is the frequency. The suffix "s" refers to the synchronous particle.

2 Adiabatic capture

RF capture process for CRing is one of the main causes of beam loss in longitudinal motion. An adiabatic capture method is used for reducing the beam loss and increasing the capture efficiency. After the barrier bucket accumulation, the beam in CRing can be considered as a coasting beam. The initial distribution in longitudinal phase space generated by ESME is random uniform in phase θ, Gaussian in energy spread ΔE with a momentum spread of $\pm 5\times 10^{-4}$ at 2σ, see in Fig. 2. The process is called adiabatic when the relative change in bucket height or bucket area is much slower than the synchrotron frequency.

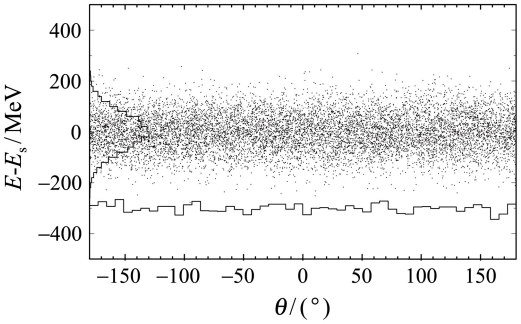

Fig. 2 Initial distribution in phase-energy space.

We introduce an adiabatic parameter $n_{\rm ad}$[4] to measure the slowness of the relative change of bucket height with respect to the synchrotron frequency:

$$n_{\rm ad}=\frac{\omega_{s0}\cdot t}{1-\sqrt{\frac{V_{\rm i}}{V(t)}}} . \tag{2}$$

where $\omega_{\rm s0}$ is the initial synchrotron frequency, $V_{\rm i}$ is the initial capture voltage. The larger the adiabatic parameter is, the more adiabatic the capture is.

From the Eq. (2), we know that $n_{\rm ad}$ is a constant at every time, and it is tenable when time comes to $t=t_{\rm cap}$. At this time the RF voltage becomes $V_{\rm f}$, the final capture voltage. Then we achieve the formula calculating $n_{\rm ad}$:

$$n_{\rm ad}=\frac{\omega_{\rm s0}\cdot t_{\rm cap}}{1-\sqrt{\frac{V_{\rm i}}{V_{\rm f}}}} . \tag{3}$$

The RF voltage program for adiabatic capture can be easily derived by solving Eqs. (2) and (3).

$$V(t)=\frac{V_{\rm i}}{\left[1-\left(1-\sqrt{\frac{V_{\rm i}}{V_{\rm f}}}\right)\frac{t}{t_{\rm cap}}\right]^2} . \tag{4}$$

There are three parameters we can change to define the RF voltage program, the capture time $t_{\rm cap}$, the initial capture voltage $V_{\rm i}$ and the final capture voltage $V_{\rm f}$.

The $V_{\rm f}$ can provide a final bucket area $A_{\rm B}$ which is large enough to restrain particles in the stationary bucket. We set that bucket area $A_{\rm B}$ and bunch area $A_{\rm b}$ has a relationship $A_{\rm B}/A_{\rm b}=3/2$. So that the bucket which $V_{\rm f}$ builds at the end of capture process will cover all particles in the bunch theoretically in consideration of the growth of momentum spread.

$V_{\rm f}$ and $A_{\rm b}$ can be derived according to the following formulas respectively[5]:

$$A_{\rm b}=2\pi\times 2\frac{\Delta E}{\omega_{\rm si}}\ , \tag{5}$$

$$V_{\rm f}=\left(\frac{A_{\rm B}}{16}\right)^2\frac{2\pi h|\eta|\omega_{\rm s}^2}{q\beta^2E_{\rm s}}\ . \tag{6}$$

In order to decrease the influence from the non-adiabatic process at $t=0$, where there is an abrupt change of RF voltage from zero up to $V_{\rm i}$, a voltage of 0.176 kV is appropriate taking the respond speed of the electronic devices into consideration. In other words, we make the initial capture voltage and final capture voltage satisfy a relationship $V_{\rm i}/V_{\rm f}=1/30$. Then we change the capture time only to find a best value which is good enough to capture the accumulated beam. Fig. 3 gives the simulation results after capture process with capture time 30, 50, 80 and 120 ms respectively. We find that the capture time of 80 ms is good enough which is neither too short to cause beam filamentation nor too long to increase the chance of beam losing. The capture time of 120 ms is not necessary because the particle distribution is almost the same comparing with 80 ms which is much longer compare to the synchrotron period $T_{\rm s}$[5]. The synchrotron period has a form as below:

$$T_{\rm s}=\tau_0\sqrt{\frac{2\pi\beta^2E}{eV_0\ h\eta}}\ , \tag{7}$$

where E is the injection energy, V_0 =5.284 kV, and τ_0 is the circulating period about several microseconds in general.

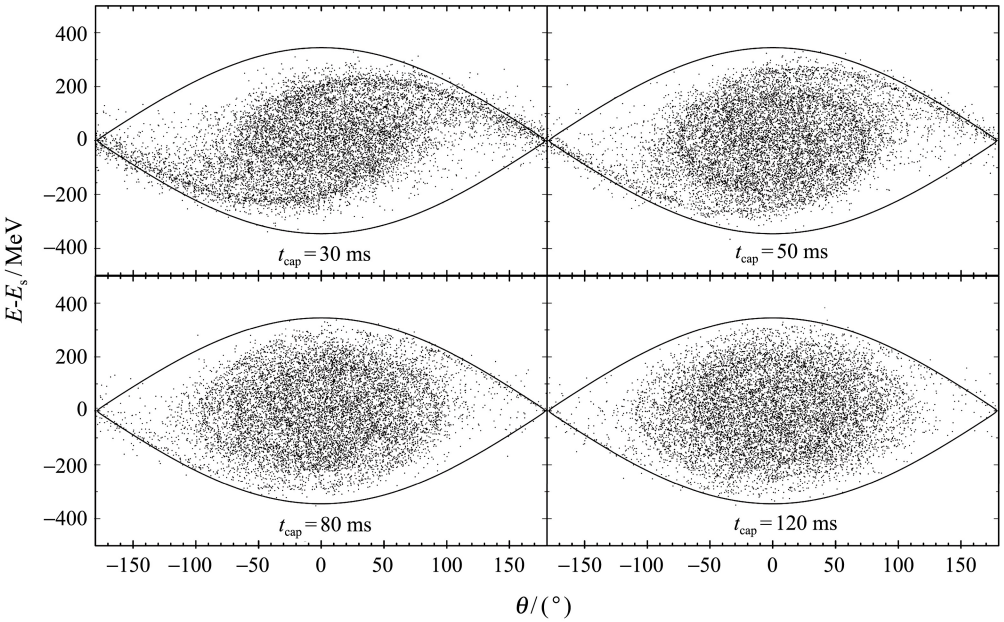

Fig. 3　Simulation results with different capture time.

In the capture process, the RF system with the zero phase all the time provides a perfect matching of the stationary bucket for the accumulated beam. The time-varying parameters such as magnetic field and RF frequency keep constant. A capture efficiency of 99.3% is achieved from the simulation results (see Fig. 3) with choosing appropriate parameters in CRing, as listed in Table 2. Compared with the adiabatic capture efficiency of 70% which is investigated in CSRm[6], a higher efficiency is achieved.

Table 2　Adiabatic capture, relevant parameters.

Parameter	Sign&unit	Value
Num. of particles	N	10 000
Capturing energy	$E_{\rm i}$/(MeV/u)	800
Bunch area	$A_{\rm b}$/eVs	931.74
Bucket area	$A_{\rm B}$/eVs	1 397.61
Initial capture voltage	$V_{\rm i}$/kV	0.176
Final capture coltage	$V_{\rm f}$/kV	5.284
Capture time	$t_{\rm cap}$/ms	80
Adiabatic parameter	$n_{\rm ad}$	32

Continued Table 2.

Synchrotron period	T_s/ms	19.20
Filling factor	A_b/A_B	0.666
Capture field	B_{cap}/T	1.7835

3 Optimization of acceleration efficiency

After adiabatic capture process, the coasting beam is changed into one bunch and we get a Gaussian like distribution in both E and θ directions, see in Fig. 4. We keep the harmonic number $h=1$ at the beginning of acceleration.

This section describes the basic theory we used to optimize the acceleration efficiency and shows the simulation results of acceleration. The energy of synchronous particle will be accelerated from 800 to 1 130 MeV/u.

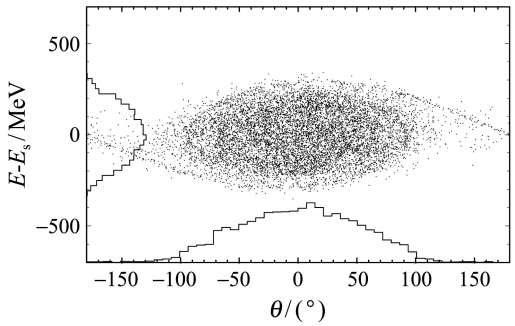

Fig. 4 Initial distribution for acceleration.

3.1 Method of optimization

In general, the particle energy must synchronize with the magnetic field generated by dipole strictly to keep the synchronous particle moving on a closed orbit. We use the difference Eqs. (8)[7] to supersede the Eqs. (1), which means we calculate the energy and phase of particles turn by turn. One equation gives the phase slip between an individual particle and a synchronous particle during the passage between RF gaps, and one gives the energy change at the gap:

$$\begin{cases} \delta_{n+1} = \delta_n + \dfrac{q}{\beta^2 E_s}\left[V(\theta) - V(\theta_s)\right] \\ \theta_{n+1} = \theta_n + 2\pi h \eta \delta_{n+1} \end{cases} . \tag{8}$$

In order to get a good acceleration efficiency, the RF voltage was determined by two criteria.

(1) The energy gain of a particle must match the increase of bending magnetic field, in other words, the RF voltage V_{rf} has to satisfy the relationship below[8]:

$$V_{rf}\sin(\theta_s) = 2\pi\rho R\dot{B} . \tag{9}$$

$\dot{B}$ is the ramping rate, *i.e.* bending magnetic field changing with time.

(2) The RF bucket area A_B has to be greater than or equal to the longitudinal beam emittance A_b. In this paper, we set the relationship that

$$A_B/A_b = \frac{3}{2} . \tag{10}$$

as same as the capture process. This is not the only way to provide an acceleration bucket which is large enough to bound most particles. Other schemes can be effective in acceleration too (see Ref. [9]).

We can easily get the RF bucket area A_B if we know the longitudinal beam emittance A_b which we can calculate with a uniform distribution at injection, see in Eq. (5).

We can achieve another relationship between V and θ_s in $(\theta, \Delta E/\omega_s)$ phase space using the Eq. (11)[10].

$$A_B = 16\sqrt{\frac{qV\beta^2 E_s}{2\pi h|\eta|\omega_s^2}}\alpha_b(\theta_s) . \tag{11}$$

Here $\alpha_b(\theta_s)$ is the ratio of the bucket area between a running bucket ($\theta_s \neq 0$) and a stationary bucket ($\theta_s = 0$). Note that $\alpha_b(\theta_s)$ can be approximated by a simple function[11]:

$$\alpha_b(\theta_s) \approx \frac{1-\sin\theta_s}{1+\sin\theta_s} . \tag{12}$$

Then we have the equation:

$$A_B = 16\sqrt{\frac{qV_{rf}\beta^2 E_s}{2\pi h|\eta|\omega_s^2}}\left[\frac{1-\sin\theta_s}{1+\sin\theta_s}\right] . \tag{13}$$

Every moment we know $\dot{B}$ and A_B during acceleration, we can calculate the parameters of the synchronous particle such as E_s, ω_s, β and η. Then we can derive a simple cubic equation in either V or θ_s by solving Eqs. (9) and (13)[5]. A small program was built in Fortran to get the V or θ_s by giving $B(t)$ and A_B as a matter of convenience during simulation.

3.2 Acceleration simulation

The simulation requires magnetic field program $B(t)$, RF voltage program $V(t)$ and phase program $\theta_s(t)$ for the acceleration process in ESME. We shall assume that the magnetic field changes with time as follows:

$$\begin{cases} B(t) = B_{cap} + a(t-t_{cap})^3 \\ \dot{B}(t) = 3a(t-t_{cap})^2 \end{cases} . \tag{14}$$

This model has been used in AGS Booster to define the magnetic field cycle and ramping rate cycle both[12]. The magnetic field and ramping rate have a shape as shown in Fig. 5.

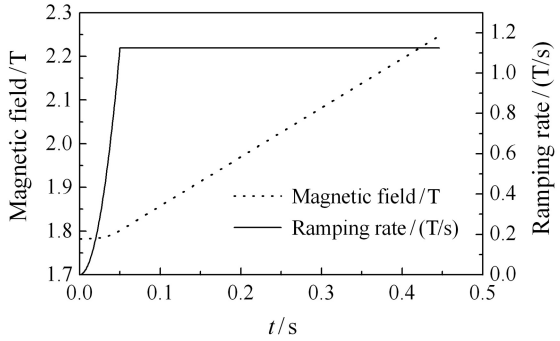

Fig. 5　Magnetic field and Rumping rate cycle.

The parameter a is chosen when $\dot{B}$ reaches the maximum value $\dot{B}^*$ at time t^*. Thus

$$a = \frac{\dot{B}^*}{3(t^* - t_{\rm cap})^2} \ . \tag{15}$$

Table 3 shows the relevant parameters in acceleration process. From the table we notice that the RF voltage at the start of acceleration is the same as the final capturing voltage. By this arrangement, we can ensure that the RF voltage changes smoothly without breaking in the actual implementation.

Table 3　Acceleration, relevant parameters.

Parameter	Sign & unit	Value
Num. of particles	N	9 925
Acceleration duration	$t_{\rm acc}$/ms	446
Max. value of $\dot{B}$	$\dot{B}^*$/(T/s)	1.125
Corresponding time point	t^*/ms	50
Corresponding RF voltage	V^*/kV	37.7
Corresponding phase	$\theta_{\rm s}^*$/(°)	27.3
Voltage at the start of this process	$V_{\rm start}$/kV	5.284
Voltage at the end of this process	$V_{\rm end}$/kV	32.7
Coefficient	a/(T/s^2)	150

Fig. 6 represents the variation tendency of RF voltage $V(t)$ (dash line), as well as synchronous phase $\theta_{\rm s}(t)$ (solid line) and RF frequency $f(t)$ (dot line) in RF cavity respectively. We see that the RF voltage has a maximum value when $B(t)$ reaches the maximum value $\dot{B}^*$.

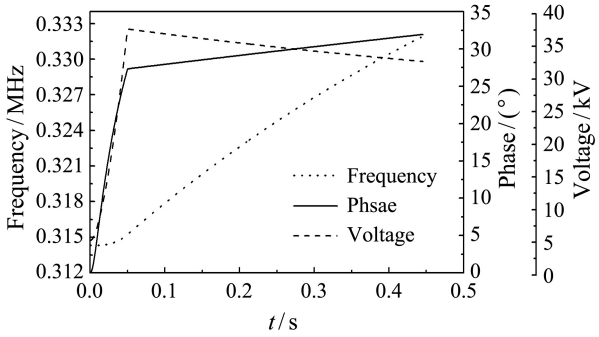

Fig. 6　The RF parameter programs used in acceleration process.

The simulation results of this process are shown in Fig. 7. Compare Fig. 7 -[(a)-(c)] with Fig. 7 -[(d)-(f)], we see that the bucket shape changes a lot before t^* when the ramping rate reaches its maximum value $\dot{B}^*$.

After about 446 ms acceleration, the beam is accelerated up to 1 130 MeV/u successfully. Almost all 9 925 particles after capture survive at the end of acceleration. So we know the acceleration efficiency is about 100% theoretically.

In Fig. 8, the distribution at $t = 0$ ms represents the particle distribution at the end of acceleration process, as well as the beginning of the debunching process.

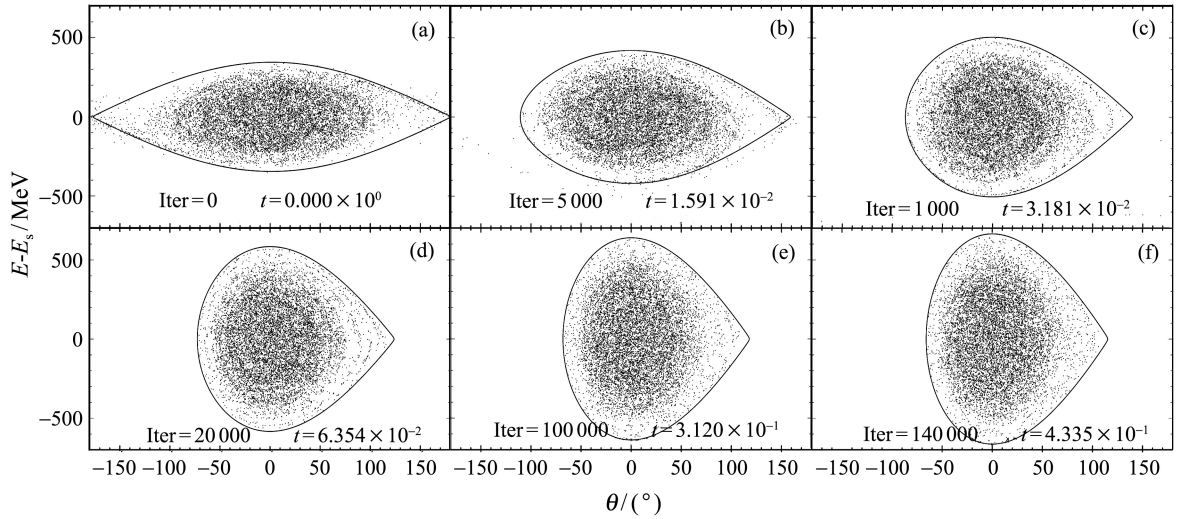

Fig. 7　Particle distribution of acceleration process using ESME program.

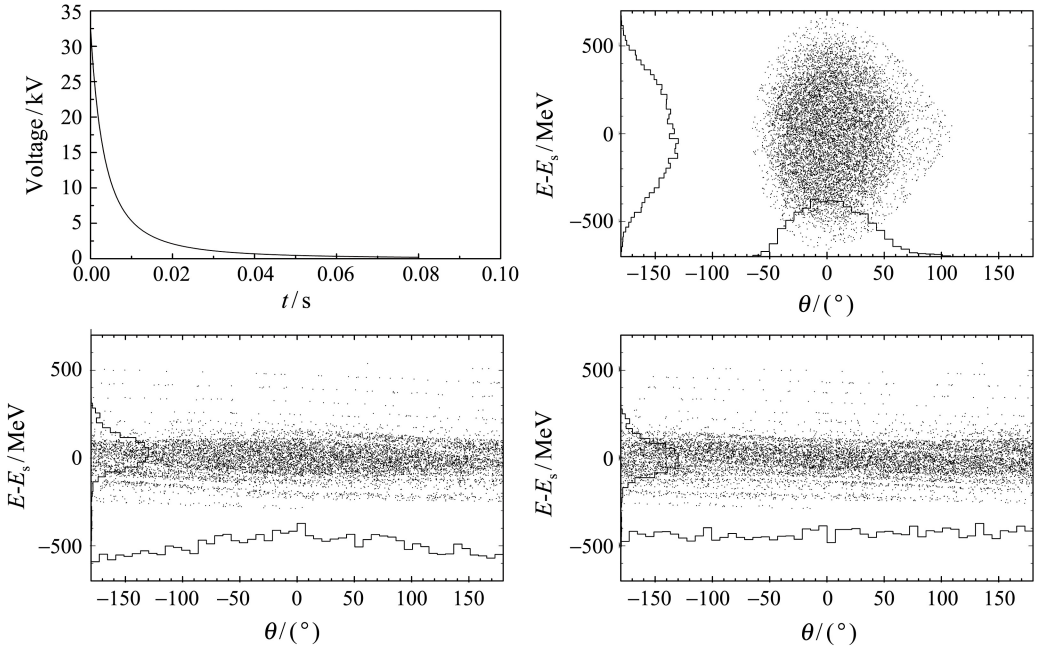

Fig. 8 Debunching process result in the end.

4 Debunching

There are two fundamental purposes of the debunching process. Firstly, the beam momentum spread can be reduced dramatically by adiabatic debunching, see in Fig. 8. The smaller the momentum spread is in debunching process, the shorter the bunch length can reach in compression process. Secondly, the frequency of RF cavity for compression is pretty high (more than 0.6 MHz), so we set the harmonic number $h = 2$ to meet the requirement of compression cavity frequency in the following compression process.

According to the adiabatic capture process, similar logic can result in the voltage program of adiabatic debunching. The initial debunching voltage should be 32.7 kV, maintaining continuous change of the RF voltage. After 80 ms, the RF voltage reaches the final debunching voltage 0.2 kV adiabatically. Then the RF can be shut down for another 20 ms to get a more uniform distribution in phase direction.

In this way we turn the one bunch beam cycling in CRing into a coasting beam with smaller momentum spread. After the beam rebunching with $h = 2$, the coasting beam can be rebunched into two bunches.

5 Conclusion

We have used the code ESME to simulate the capture process, the acceleration process and the debunching process for $^{238}U^{34+}$ beam. The beam and machine parameters are expected to be optimized for beam compression of heavy ion beams in CRing.

We have shown that capture efficiency can be improve to 99.3% with adiabatic capture program, and a 100% acceleration efficiency can be achieved using the optimum programs. Another adiabatic process is used in debunching the beam.

The RF voltage programs in capture process, acceleration process and debunching process make up a complete RF voltage cycle. In one RF cycle, the voltage increases from 0 to 5.284 kV for capturing particles into a bunch. Then, the voltage rises to 32.7 kV with an inflection point of 37.7 kV in acceleration process. Finally it drops to 0.2 kV adiabatically and shut down to 0 kV again to debunch the beam bunch. The RF voltage cycle is shown in Fig. 9 .

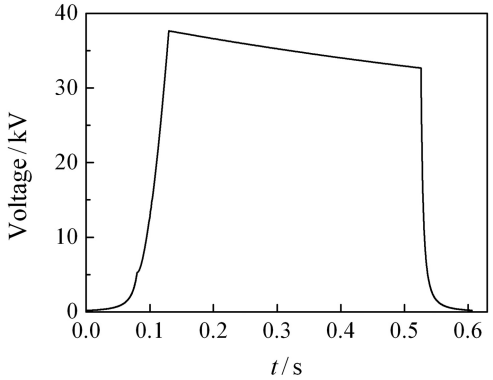

Fig. 9 The RF voltage cycle.

Simultaneously, we have shown that the maximum RF voltage we used is 37.7 kV, and the peak voltage of the RF cavity in HIAF-CRing is designed to 40 kV,

which can satisfy the RF requirement in both capture and acceleration processes.

Future work will concentrate on space charge effect to high current beams during capture and acceleration process. More precise results will be carried out considering the beam collective effects.

References:

[1] YANG Jiancheng, XIA Jiawen, XIAO Guoqing, *et al*. Nucl Inst Meth B, 2013, **317**: 263.

[2] MACLACHLAN J, OSTIGUY J F. User's Guide to ESME es2011_4.5[M]. 2011.

[3] LEE S Y. Accelerator Physics[M]. 2nd Ed. Singapore: World Scientific, 1999: 242.

[4] NG K Y. Adiabatic Capture and Debunching. FERMILAB-FN-0943-APC, 2012.

[5] HULSMANN P, FRANKEENHEIM O, KLINGBEIL H, *et al*. Considerations Concerning the RF System of the Accelerator Chain SIS12/18-SIS100 for the FAIR-project at GSI. Internal Note 2004.

[6] LIU Wei, XIA Jiawen, ZHANG Wenzhi, *et al*. High Energy Physics And Nuclear Physics, 2004, **28**(1): 92.

[7] LIU Wei, XIA Jiawen, ZHANG Wenzhi, *et al*. High Power Laser and Particle Beams, 2005, **17**: 943.

[8] LEE S Y. Accelerator Physics[M]. 2nd Ed. Singapore: World Scientific, 1999: 247.

[9] CRESCENTI M,KNAUS P,ROSSI S. The RF Cycle of the PIMMS Medical Synchrotron. No. CERN-PS-2000-032-DR. 2000.

[10] DOME G. Theory of RF Acceleration[C]//TURNER S. Cas Cern Accelerator School Advanced Accelerator Physics. Geneva: Cern, 1987, Vol.1: 110-158.

[11] LEE S Y. Accelerator Physics[M]. 2nd Ed. Singapore: World Scientific, 1999: 253.

[12] GARDNER C J. RF Capture and Acceleration of Gold Ions in Booster,C-A Department Accelerator Physics Note C-A/AP/7, November, 1999.

HIAF-CRing中的俘获加速效率研究

商 鹏[1,2]，殷达钰[1]，夏佳文[1]，杨建成[1]，曲国峰[1,2]，郑文亨[1,2]，李钟汕[1,2]，阮 爽[1,2]

（1. 中国科学院近代物理研究所，兰州 730000；
2. 中国科学院大学，北京 100049）

摘要： 以HIAF-CRing上典型离子$^{238}U^{34+}$为研究对象，对其纵向俘获和加速的动力学过程进行了研究。累积后的粒子能量为800 MeV/u, 经过绝热俘获和加速后，粒子被加速至1 130 MeV/u。研究结果表明，通过选择适当的俘获时间、绝热参数以及相空间面积因子等参数，应用优化后的高频俘获加速曲线，可以获得更高的俘获和加速效率。通过粒子纵向动力学追踪软件ESME 上进行模拟，得到了优化后的高频相位、高频电压曲线，使得俘获效率达到99.3%，加速效率近乎100%。同时确定出了CRing 高频腔加速U^{34+} 所需满足的特性参数，即电压需达到40 kV，频率范围是0.31～0.34 MHz。

关键词： 模拟；HIAF；压缩；绝热俘获；加速

收稿日期： 2014-11-14；　**修改日期：** 2015-01-08

通信作者： 殷达钰，E-mail: yindy@impcas.ac.cn。